

Cross-platform transcriptomic profiling of the response to recombinant human erythropoietin

Guan Wang (✉ g.wang2@brighton.ac.uk)

University of Brighton

Traci Kitaoka

Illumina (United States)

Ali Crawford

Illumina (United States)

Qian Mao

BGI Group (China)

Andrew Hesketh

University of Brighton

Fergus Guppy

University of Brighton

Garrett Ash

Yale University

Jason Liu

Yale University

Mark Gerstein

Yale University

Yannis Pitsiladis

University of Brighton

Research Article

Keywords: RNA biology, MGI DNBSEQ™, BeadChip, GeneChip™, Human Transcriptome Array 2.0

Posted Date: May 19th, 2021

DOI: <https://doi.org/10.21203/rs.3.rs-510750/v1>

License: © ⓘ This work is licensed under a Creative Commons Attribution 4.0 International License.

[Read Full License](#)

1 **Cross-platform transcriptomic profiling of the response to recombinant**
2 **human erythropoietin**

3
4 Guan Wang^{1,2*}, Traci Kitaoka³, Ali Crawford³, Qian Mao⁴, Andrew Hesketh⁵, Fergus M.
5 Guppy^{5,6}, Garrett I. Ash^{7,8}, Jason Liu⁹, Mark B. Gerstein⁹⁻¹², Yannis P. Pitsiladis^{6*}
6

7 ¹Sport and Exercise Science and Sports Medicine Research and Enterprise Group, University of
8 Brighton, Brighton, UK.

9 ²Centre for Regenerative Medicine and Devices, University of Brighton, Brighton, UK.

10 ³Illumina, San Diego, CA, USA.

11 ⁴BGI, Shenzhen, China.

12 ⁵School of Pharmacy and Biomolecular Sciences, University of Brighton, Brighton, UK.

13 ⁶Centre for Stress and Age-related Disease, University of Brighton, Brighton, UK.

14 ⁷Veterans Affairs Connecticut Healthcare System, West Haven, CT, USA.

15 ⁸Center for Medical Informatics, Yale University, New Haven, CT, USA.

16 ⁹Program in Computational Biology & Bioinformatics, Yale University, New Haven, CT, USA.

17 ¹⁰Department of Molecular Biophysics & Biochemistry, Yale University, New Haven, CT, USA.

18 ¹¹Department of Computer Science, Yale University, New Haven, CT, USA.

19 ¹²Department of Statistics and Data Science, Yale University, New Haven, CT, USA.

20 *Corresponding authors. Email: g.wang2@brighton.ac.uk; y.pitsiladis@brighton.ac.uk.

21 **Abstract**

22 RNA-seq has matured and become an important tool for studying RNA biology. Here we
23 compared two RNA-seq (Illumina sequencing by synthesis and MGI DNBSEQTM) and two
24 microarray platforms (Illumina Expression BeadChip and GeneChipTM Human Transcriptome
25 Array 2.0) in healthy individuals administered recombinant human erythropoietin for
26 transcriptome-wide quantification of differential gene expression. The results show that total
27 RNA sequencing combined with DNB-seq produced a multitude of genes of biological relevance
28 and significance in response to recombinant human erythropoietin, in contrast to other platforms.
29 Through data triangulation linking genes to functions, genes representing the processes of
30 erythropoiesis as well as non-erythropoietic functions of erythropoietin were unveiled. This
31 study provides a knowledge base of genes characterising the responses to recombinant human
32 erythropoietin through cross-platform comparison and validation.

33

34 **Introduction**

35 High-throughput technologies in gene discovery, quantification and functional investigation have
36 advanced our understanding of complex traits and facilitated disease diagnosis, prevention and
37 treatment over the past decade^{1, 2}. Although technologies continue to evolve for discerning and
38 characterising genes and gene-protein interactions both *ex-* and *in-vivo*, uncovering coding
39 transcriptomes of bulk cells can capture global gene expression patterns that may directly
40 pinpoint important biological processes at the molecular level. Which tool to use will ultimately
41 depend on the fundamental research question. Here, we performed RNA-seq and microarray
42 analyses in healthy individuals administered recombinant human erythropoietin (rHuEPO) to
43 assess their discriminatory capacity, and importantly, to explore the implications of the findings
44 to better understanding the systemic responses to rHuEPO; a first of its kind in the investigation
45 of transcriptome-wide responses to rHuEPO in humans. This study primarily differs from
46 previous cross-platform gene-expression studies in 1) systematic comparisons between two
47 RNA-seq platforms (MGI DNBSEQ-G400RS and Illumina NextSeq 500), 2) comparisons with
48 the benchmarking microarrays (GeneChipTM Human Transcriptome Array 2.0 and Illumina
49 HumanHT-12 v4 Expression BeadChip), 3) the use of a relatively large number of the same
50 experimental samples across all four platforms, and 4) the adoption of a data triangulation
51 approach across platforms to prioritise the functional genes of diagnostic potential.

52
53 Eighteen endurance-trained Caucasian males at sea level (Glasgow, Scotland; age: 26.0±4.5 yrs,
54 weight: 74.8±7.9kg, height: 179.8±5.4cm) underwent 4 weeks of rHuEPO injections (50 IU/kg
55 every 2 days)³. Whole blood samples collected from the 18 subjects across 8 time points —
56 before (−14- and −1-day prior to the first injection; Base1 and Base2), during (2-, 14- and 28-day

57 into the administration; EPO3, EPO4 and EPO5) and post rHuEPO administration (2-, 14- and
58 28-day after the last injection; Post6, Post7 and Post8) — were analysed on the Illumina
59 HumanHT-12 v4 Expression BeadChip previously⁴. In the current study, 50 samples from 10 of
60 the 18 subjects collected at Base1, Base2, EPO3, EPO4 and Post7 were analysed on the two
61 RNA-seq platforms as well as on the GeneChipTM array for quantifying differential gene
62 expression (DGE). This experimental design aimed to identify the gene expression response to
63 rHuEPO through robust quantification processes, and to generate results with wide applications
64 ranging from developing effective therapeutics targeting clinical disorders associated with EPO
65 dysfunctions to facilitating sensitive testing strategies against blood doping in sport.

66

67 **Results**

68 **Total RNA DNB-seq (MGI) identifies a wealth of mRNA genes in response to rHuEpo**

69 We identified 16,738 genes (MGI RNA-seq), 16,581 genes (Illumina RNA-seq), 29,517
70 transcript clusters (GeneChip), and 10,622 transcripts (BeadChip) for the DGE analyses (Table
71 1). Both MGI and Illumina RNA-seq generated good base call quality, with an average quality
72 score of >34 across the read lengths and across the samples (Supplementary Fig. 1). No sample
73 contamination/swaps (Supplementary Fig. 2) and no other significant surrogate variables of
74 batch effects were detected in these sequencing datasets. Genome mapping using HISAT2⁵
75 (against the reference genome assembly GRCh38.p12⁶) showed the overall alignment rates of
76 94.2% (MGI; 197.9M total reads) and 95.0% (Illumina; 110.4M total reads) (Supplementary
77 Table 1). RseQC⁷ revealed a large proportion of the sequences aligned to introns in the MGI
78 RNA-seq data (37.4% versus 8.7% Illumina on average; Supplementary Fig. 3 and
79 Supplementary Table 2), a result coinciding with the differing sequencing library preparation

80 methods used (total RNA-seq with rRNA depletion and globin mRNA reduction, MGI versus
81 mRNA enrichment, Illumina). RseQC also showed that among a total of 186.6M (MGI) and
82 104.6M (Illumina) averaged reads observed, 52.4% (~ 97.8M reads) and 74.8% (~ 78.2M reads)
83 of the reads were effectively mapped to the coding sequences (exons), respectively
84 (Supplementary Table 2). The average Salmon⁸ transcriptome mapping rates, following
85 selective-alignment-based lightweight mapping, were 38.8% (38.3M aligned reads; MGI) and
86 81.9% (45.1M aligned reads; Illumina) (Supplementary Table 3). The seeming discrepancies
87 observed in total reads and alignment rates across the software tools (HISAT2, RseQC and
88 Salmon) were expected given their specific usage. Overall, these data suggested high quality
89 sequences obtained from both sequencing platforms. For the purposes of cross-platform
90 comparison, the relative abundance estimates of transcripts after Salmon transcriptome mapping
91 were summed to gene level, and genes were considered expressed when the gene-level
92 abundance estimates were equal to or more than 5 in at least 4 samples; resulting in the exclusion
93 of 17,198 and 18,347 genes from the MGI and Illumina RNA-seq datasets, respectively (Table
94 2). Gene annotation resulted in 3,852 (MGI) and 2,860 (Illumina) un-defined gene mappings
95 removed from the sequencing datasets (Table 2). As a result, 16,738 and 16,581 protein-coding
96 genes identified from MGI and Illumina sequencing, respectively, were used for the downstream
97 DGE analyses (Table 1 and 2).

98
99 Initial quality control metrics revealed variability in eight out of the fifty GeneChipTM arrays
100 (Supplementary Fig. 4A). Two of the eight samples were then repeated for chip scanning, and
101 the other six samples were repeated from the target preparation step (Supplementary Fig. 4B).
102 Raw intensity values obtained from the GeneChip and BeadChip analyses correspond to 67,480

103 and 47,286 coding and non-coding transcriptomic features, respectively (Table 1). The process
104 of normalisation and filtering unveiled 29,517 transcript clusters (GeneChip) and 10,622
105 transcripts (BeadChip) as identified features (Table 1), with the detailed filtering steps and the
106 resulting number of features summarised in Table 2. Briefly, 18,494 and 6,900 probes were
107 removed as undetected and low-quality probes, respectively, from the BeadChip dataset (Table
108 2). While 8,166 probes were removed due to low average expression (cutoff value: 5.1) in the
109 BeadChip dataset, no such probes were necessarily excluded from the GeneChip dataset
110 (Supplementary Fig. 5 and Table 2). No significant surrogate variables representing the
111 underlying biases, potentially arising from library preparation and/or scanning, thereby
112 confounding the biological effects being studied, were observed in the two microarray datasets.

113

114 Unsupervised principal component analysis (PCA) revealed substantial variance, estimated using
115 the top 500 genes ranked by expression variance across all samples. Variances explained by the
116 principal component 1 and the principal component 2 were: 69% vs. 5% (MGI RNA-seq), 44%
117 vs. 9% (Illumina RNA-seq), 58% vs. 14% (GeneChip), and 78% vs. 7% (Beadchip)
118 (Supplementary Fig. 6). Gene clustering of the top 30 genes of high variance showed a good
119 distinction across biological conditions in all datasets (Supplementary Fig. 7). Nevertheless, a
120 more distinctive pattern across the conditions was observed following MGI RNA-seq compared
121 to Illumina RNA-seq and GeneChip (Supplementary Fig. 7, A versus B, C). In contrast with the
122 discrimination pattern presented in the 143 BeadChip samples, a higher expression level of the
123 examined top 30 genes was detected by MGI RNA-seq (Supplementary Fig. 7, A versus D). The
124 DESeq⁹ and limma¹⁰ DGE analyses yielded 1,552, 582, 252 and 2,372 transcriptomic features
125 exceeding the pre-defined thresholds following MGI RNA-seq, Illumina RNA-seq, GeneChipTM

126 and BeadChip, respectively (thresholds for RNA-seq: a fold change of 1.2 and *s*-value of 0.005;
127 for microarray: a fold change of 1.2 and BH adjusted *p*-value of 0.05; note that the probability
128 thresholds bound to the fold change of 1.2) (Table 3). A significant proportion of these findings
129 were unique to MGI RNA-seq at EPO4 (66.8%) and Post7 (54.5%) (Supplementary Table 4).
130 Notably, substantial sub-proportions of the gene features identified from MGI RNA-seq
131 exceeded an absolute fold change of 2 (12.4% at EPO4 and 18.0% at Post7) and captured even
132 smaller changes between 1.2 and 2 (54.4% at EPO4 and 36.5% at Post7), when compared to the
133 Illumina RNA-seq and GeneChipTM gene features (ranging from 0% to 19.4%; Supplementary
134 Table 4 and Fig. 1). Furthermore, strong correlations between the two RNA-seq platforms on the
135 commonly identified genes were observed ($r = 0.74$ at EPO4 and $r = 0.85$ at Post7, $P < 2E-16$;
136 Fig. 2, a and d), whereas the correlations ranged from very weak ($r = 0.2$) to moderate ($r = 0.7$)
137 when compared RNA-seq to GeneChipTM ($P < 0.0003$; Fig. 2, b, c, e and f). Overall, MGI RNA-
138 seq, the total RNA DNB-seq, resulted in an increased sensitivity in identifying coding genes in
139 response to EPO compared to the Illumina mRNA-seq and GeneChipTM (Fig. 1, Fig. 2 and
140 Supplementary Data 1).

141

142 **Pathway analysis links the differentially expressed genes to erythropoiesis and non-** 143 **erythropoietic functions of EPO**

144 To explore the biological functions of the gene features identified from sequencing and
145 microarray, we performed a standard GSEA run (v4.0.3) subject to 1,000 phenotype
146 permutations^{11, 12} on all datasets, using the MSigDB (v7.2)^{11, 13} hallmark (H)¹⁴ and Gene
147 Ontology (C5; BP: GO biological process)^{15, 16} collections of functional gene sets. As expected,
148 heme metabolism emerged as the most significantly enriched pathway in all datasets following

149 the analysis on the 50 hallmark gene sets (FDR: MGI = 0.011 EPO4, Illumina = 0.033 EPO4,
150 GeneChip \leq 0.017 EPO4/Post7 and BeadChip \leq 0.004 EPO3/4/5/Post7/8; Supplementary Table
151 5). Leading edge genes, those contributing the most to the enrichment score of the heme
152 metabolism pathway constituting 200 genes, included 144 (MGI; EPO4), 105 (Illumina; EPO4),
153 125/96 (GeneChip; EPO4/Post7) and 101/103/103/97/84 (BeadChip; EPO3/4/5/Post7/8) genes
154 found in these datasets (Supplementary Data 2). Fifty-six leading edge genes overlapped across
155 all platforms and across conditions (pathway FDR < 0.1) (Supplementary Data 2). Of the 56
156 genes, 51 and 34 genes were also identified by the standard DGE analyses for the EPO4 and
157 Post7 conditions, respectively, across two or three of the MGI RNA-seq, Illumina RNA-seq and
158 GeneChip™ platforms (Supplementary Data 3). GSEA was able to detect the associated genes
159 that have fallen off the detection thresholds in the standard DGE analyses of Illumina RNA-seq
160 and GeneChip datasets (Supplementary Data 3). In addition, subsets of 10, 51, 51, 36, and 19 of
161 the 56 leading edge genes were found in the BeadChip DGE results across EPO3, EPO4, EPO5,
162 Post7 and Post8 conditions, respectively (Supplementary Data 4). The data suggest the
163 effectiveness of all four detection platforms and the effectiveness of GSEA in capturing the most
164 context-relevant biological pathway in response to rHuEPO. Next, GSEA was conducted on
165 7,530 GO biological processes included in the MSigDB C5 collection, and identified a total of
166 212, 134, and 33 biological pathways from MGI RNA-seq (EPO4), GeneChip (EPO4) and
167 BeadChip (EPO4, EPO5, Post7 and Post8) datasets, respectively, exceeding the pathway FDR <
168 0.1 and nominal $P < 0.05$. No significantly enriched GO biological processes were identified
169 from GSEA in the Illumina RNA-seq datasets. From the MGI RNA-seq dataset, these included
170 biological processes, resembling EPO cytoprotective functions and the downstream signal
171 transduction pathways¹⁷⁻¹⁹, typically involved in response to oxidative stress (e.g. positive

172 regulation of mitophagy, hydrogen peroxide metabolic process, and nucleotide-excision repair,
173 DNA damage recognition), heme formation (e.g. porphyrin-containing compound metabolic
174 process), erythrocyte development, mTOR (target of rapamycin) signaling, regulation of energy
175 metabolism (e.g. regulation of generation of precursor metabolites and energy), low density
176 lipoprotein clearance, and nervous system development (Fig. 3). Key pathways characterising the
177 responses to EPO, such as autophagy of mitochondrion, positive regulation of cell cycle arrest,
178 iron ion homeostasis, tetrapyrrole metabolic process, erythrocyte development, and ventricular
179 system development also were identified from the GeneChip dataset (Supplementary Fig. 8). In
180 addition, other biological processes, including cyclic GMP mediated signaling, positive
181 regulation of cardiac muscle cell proliferation, and gamma-aminobutyric acid transport, were
182 observed, to name a few (Supplementary Fig. 8). In the BeadChip datasets, particular pathways
183 identified that were common to those observed on both the MGI RNA-seq and the GeneChip
184 platforms included hemoglobin metabolic process, erythrocyte development, and hydrogen
185 peroxide metabolic process (Supplementary Fig. 9). Further pathways of negative regulation of
186 necrotic cell death, negative regulation of TORC1 signaling, cellular response to monoamine
187 stimulus, monoamine transport, gas transport, lipid transport, drug transmembrane transport,
188 synaptic signaling, synapse organisation, and multicellular organism development, were found in
189 the BeadChip datasets (Supplementary Fig. 9). Leading edge genes from top 34, 14, and 16
190 pathways defined by the normalised enrichment score (NES) > 1.90 and from 38, 66, and 12 the
191 most enriched pathways representing a biological theme where NES < 1.90 were further
192 investigated in the MGI RNA-seq, GeneChip and BeadChip datasets, respectively. Out of a total
193 of 308 leading edge genes identified in the MGI RNA-seq EPO4 dataset overlapping with the
194 DESeq2 EPO4 DGE results, 135 genes also were found to be significantly expressed in the Post7

195 condition following the DESeq2 analysis (Supplementary Data 5). Of the 135 genes, top 10
196 genes filtered based on the GSEA ranks and pathway NESs — *BPGM*, *ALAS2*, *PKD1L3*,
197 *SLC4A1*, *AP2A1*, *IGF2*, *FAM210B*, *DYRK3*, *FECH* and *SLC25A37* — characterise erythrocyte
198 development, heme formation, metal ion homeostasis, cellular response to PH, LDL particle
199 clearance, glucose and energy metabolism, and TOR signaling (Supplementary Data 5). Fifty-
200 seven leading edge genes of the GeneChip EPO4 dataset were common to the limma EPO4 DGE
201 genes, while 15 (of the 57) were also present in the Post7 DGE results (Supplementary Data 6).
202 These 15 genes — *ALAS2*, *SLC4A1*, *FOXO3*, *TMOD1*, *FECH*, *SLC6A8*, *SLC25A39*, *SNCA*,
203 *FAM210B*, *EPB42*, *SLC25A37*, *YBX3*, *BPGM*, *STRADB*, and *BCL2L1* — correlate with heme
204 formation, bicarbonate transport, muscle atrophy, lens fiber cell development, gamma-
205 aminobutyric acid transport, erythrocyte development, cellular hyperosmotic response, negative
206 regulation of signal transduction in the absence of ligand and cellular response to amino acid
207 stimulus (Supplementary Data 6). Among 376 leading edge genes identified from the BeadChip
208 datasets, 76 also were observed in the limma DGE analysis. Top 10 genes (of the 76 genes) —
209 *KCNJ10*, *YBX3*, *SNCA*, *OR2W3*, *IRX1*, *OR2W5*, *CAMK2A*, *ACP4*, *NCDN* and *HOXC10* — are
210 involved in regulation of neuronal synaptic plasticity and necrotic cell death, sensory perception
211 of smell, proximal/distant pattern formation, and cell fate specification, and were enriched in the
212 GSEA Post7 dataset as well as were significantly expressed across EPO4, EPO5, Post7 and
213 Post8 conditions following the limma DGE analysis (Supplementary Data 7). Among the above
214 135, 15 and 76 leading edge genes identified on the three platforms, *BPGM*, *ALAS2*, *SLC4A1*,
215 *FAM210B*, *EPB42*, *SNCA*, *YBX3* and *TMOD1* were detected by all three platforms
216 (Supplementary Data 8). *FECH*, *SLC25A37*, *FOXO3*, *BCL2L1*, and *SLC25A39* were common
217 between MGI RNA-seq and GeneChip, *SLC6A8* between GeneChip and BeadChip, and *SLC7A5*,

218 *PINK1, DMTN, TRIM58, SESN3, GATA1, FURIN, HBQ1, EIF2AK1, and HBM* between MGI
219 RNA-seq and BeadChip (Supplementary Data 8). One hundred and twelve leading edge genes
220 (top 5: *PKDIL3, AP2A1, DYRK3, IGF2* and *TALI*) were uniquely identified by MGI RNA-seq, 1
221 (*STRADB*) by GeneChip and 57 by BeadChip (top 5: *KCNJ10, OR2W3, IRX1, OR2W5* and
222 *CAMK2A*) (Supplementary Data 8). Further, 43 leading edge genes identified from one or more
223 of the three platforms were detected by Illumina RNA-seq across EPO4 and Post7 conditions
224 following the DESeq2 DGE analysis (Supplementary Data 9).

225
226 To follow up on the DGE and GSEA results, we performed additional analysis using the
227 Reactome database to examining the pathway components inferred from the 43 genes in pathway
228 diagrams and to confirming the gene functions attributed to rHuEPO across the experimental
229 conditions. By overlaying the gene expression values on Reactome pathway diagrams (release
230 73)²⁰, 13 and 8 significantly expressed interaction networks represented by 29 and 13 of the 43
231 genes, or their interactors (IntAct score ≥ 0.556), were identified in the MGI RNA-seq and
232 BeadChip datasets, respectively (pathway FDR < 0.05; see Supplementary Data 10 for pathway
233 entities and statistics and Supplementary Data 11 for the corresponding pathway overviews).
234 Notably, pathway components in the entire cascade of O₂/CO₂ exchange in erythrocytes were the
235 most significantly altered in the MGI RNA-seq datasets as opposed to findings obtained from the
236 Illumina RNA-seq, GeneChip and BeadChip platforms, including the pathway genes *SLC4A1,*
237 *HBB, CA1, AQPI, RHAG, HBA1* and *CYBSR1* (pathway FDR ≤ 0.003 , Supplementary Data 10)
238 across EPO4, up-regulation and Post7, down-regulation (see Fig. 4 for the enhanced high-level
239 pathway diagram of the Post7 dataset). Finally, by overlapping a total of 172 and 91 significantly
240 expressed Reactome pathway genes and their interactors (IntAct score > 0.9 of high confidence

241 interactions, Supplementary Data 10) emerged from the 13 and 8 networks with the genes
242 identified from the standard DGE analyses in the MGI RNA-seq and BeadChip datasets, 80 and
243 41 genes were further confirmed, respectively (Supplementary Data 12). These 80 and 41 genes
244 represent the candidate genes that warrant further studies to rule out potential confounding
245 factors that mimic the EPO effect in terms of developing robust anti-doping gene signatures, or
246 to verify the role of the genes in EPO production and function for therapeutic purposes. The
247 subsets of the top 10 genes (sorted by the standard DGE *s*-value < 0.005 or FDR < 0.05)
248 accompanied by their corresponding GSEA and Reactome pathways are presented in
249 Supplementary Table 6 and 7.

250

251 **Discussion**

252 Taken together, cross-platform comparison in 10 subjects administered rHuEPO (50 IU every 2
253 days for 4 weeks) was conducted following gene expression quantification on MGI DNBSEQ-
254 G400RS, Illumina NextSeq 500 and GeneChipTM HTA2.0 platforms. To initiate a direct
255 comparison, only the coding gene features were extracted and compared across platforms. There
256 was a 2.28-fold increase in genes significantly expressed following MGI RNA-seq, as compared
257 to the combined number of genes identified on the other two platforms (Fig. 1 and
258 Supplementary Table 4). Furthermore, among 1,126 genes identified at EPO4, 25.5% of the
259 genes overlapped between MGI RNA-seq and the other two platforms, and 66.8% of the genes
260 were unique to MGI RNA-seq; among 674 genes identified at Post7, the corresponding figures
261 were 21.5% and 54.5%, respectively (Supplementary Table 4). Among genes with an absolute
262 fold change less than 2, Illumina RNA-seq captured a much higher proportion of the identified
263 gene features compared to GeneChip (10.3% vs 1.7% EPO4; 26.4% vs 0.6% Post7;

264 Supplementary Table 4). The experimental effect of EPO was largely captured by MGI RNA-seq
265 (PC1: 69% vs PC2: 5%), followed by GeneChip (PC1: 58% vs PC2: 14%) and Illumina RNA-
266 seq (PC1: 44% vs PC2: 9%) by examining the top 500 genes showing the highest variability
267 across samples (Supplementary Fig. 6, A to C). These observations support the supreme
268 performance of total RNA DNB-seq on MGI DNBSEQ-G400RS, followed by mRNA-seq on
269 Illumina NextSeq 500 and GeneChipTM HTA2.0 in this study. Nevertheless, genes characterised
270 by Illumina HumanHT-12 v4 Expression BeadChip in the 18 subjects represented a total of 85%
271 of variance captured by PC1 (78%) and PC2 (7%) (Supplementary Fig. 6D), suggesting
272 increased statistical power owing to the larger sample size (i.e. 143 samples from 18 subjects in
273 contrast to 50 samples from 10 subjects comprising the sample sets analysed on the other
274 platforms). Following on, quantitative pathway analysis by GSEA identified the heme
275 metabolism pathway enriched in all datasets across the four high-throughput gene quantification
276 platforms when analysing the MSigDB Hallmark collection of functional gene sets, while 212,
277 134, and 33 enriched pathways were unveiled from MGI RNA-seq, GeneChip and BeadChip
278 datasets, respectively, by examining the MSigDB C5 collection of 7,530 biological processes.
279 The pathway results underpinned the biological relevance of the gene expression findings,
280 particularly with a wealth of functional information emerged from the MGI RNA-seq dataset
281 (Fig. 3). Pathways of interest were prioritised by focusing on pathways of NES > 1.9 and
282 representative pathways of the biological themes where the NES < 1.9. Three hundred and eight,
283 57 and 376 leading edge genes were extracted from the pathways of interest, eventually led to
284 135, 15 and 76 genes also confirmed by the standard DGE analyses of MGI RNA-seq, GeneChip
285 and BeadChip datasets, respectively (Supplementary Data 5-7). Among these genes, 43 were
286 further validated in the list of genes resulted from the Illumina RNA-seq DGE analysis

287 (Supplementary Data 9). Despite strong positive correlations observed at the gene level between
288 MGI RNA-seq and Illumina RNA-seq, the lack of significantly expressed pathways following
289 GSEA in the Illumina RNA-seq datasets is in line with the generally weaker signals being picked
290 up by Illumina RNA-seq in this study (Fig. 2). To better understand the interacting networks or
291 signaling cascades represented by the 43 genes, we explored the Reactome database and
292 generated a total of 21 pathway overviews detailing the pathway entities/genes, their expression
293 levels, and their interactions with other entities within the pathway or across different pathways
294 (Supplementary Data 11). Finally, by extracting the significantly altered genes involved in these
295 Reactome networks and by matching these genes to the results of the standard DGE analyses, we
296 concluded with the lists of 80 and 41 genes that are of biological relevance to rHuEPO, identified
297 on the MGI RNA-seq and BeadChip platforms, respectively (Supplementary Data 12). They
298 represent the top biological pathways enriched in metabolism of porphyrins, O₂/CO₂ exchange in
299 erythrocytes, response to oxidative stress induced cellular senescence, and tissue damage caused
300 by amyloid deposition.

301
302 This comprehensive profiling of rHuEPO gene expression based on both RNA-seq and
303 microarrays has generated a robust set of genes of biological significance in relation to
304 erythropoiesis as well as non-erythropoietic effects of rHuEPO. It also establishes a knowledge
305 base of genes capturing a wide range of magnitude of changes attributable to rHuEPO by RNA-
306 seq, highlighting advantages of total RNA-seq combined with DNB-seq in quantifying gene
307 transcription. The adoption of a data triangulation approach by cross-platform comparisons and
308 by linking genes to their functions reinforces the biological findings and mitigates gene
309 expression perturbations caused by normal physiological changes such as seasonal changes and

310 lifestyle related changes. The longitudinal nature of the current investigation in healthy
311 individuals would help facilitate detailed studies of erythroid disorders and help formulate target
312 therapeutics, through disrupting and examining the mechanisms of the putative genes involved in
313 erythropoiesis and non-erythropoietic functions of rHuEPO. Finally, this study underpins the
314 follow-up studies needed to develop sensitive and robust gene signatures of blood doping in
315 sport.

316

317 **Methods**

318 **Subjects**

319 In a previously funded research project by the World Anti-Doping Agency (grant no.:
320 08C19YP), we collected whole blood samples from 18 endurance-trained Caucasian males at sea
321 level from Glasgow, Scotland (26.0±4.5 yrs, 74.8±7.9 kg, 179.8±5.4 cm), who underwent 4-
322 week 50 IU·kg⁻¹ body mass of rHuEPO every second day³. Daily oral iron supplementation (100
323 mg of elemental iron, ferrous sulphate tablets, Almus, Barnstable, UK) was given during the 4
324 weeks of rHuEPO administration³. Whole blood samples were collected at baseline (2 weeks and
325 1 day before rHuEPO; denoted by Base1 and Base2, respectively), during the rHuEPO
326 administration (2 days, 2 and 4 weeks following the 1st injection; denoted by EPO3, EPO4 and
327 EPO5, respectively) and for 4 weeks after the rHuEPO administration (1, 2 and 4 weeks after the
328 last injection; denoted by Post6, Post7 and Post8, respectively) for gene expression profiling on
329 the HumanHT-12 v4.0 Expression BeadChip (Illumina, San Diego, CA, USA)⁴. In the current
330 study (grant no.: ISF15E10YP), samples from 10 out of the 18 subjects collected at Base1,
331 Base2, EPO3, EPO4 and Post7 were analysed on a new microarray platform (GeneChipTM
332 Human Transcriptome Array 2.0 or HTA2.0, Thermo Fisher Scientific, Waltham, MA, USA)

333 and on two RNA-seq platforms (NextSeq500, Illumina, San Diego, CA, USA, and DNBSEQ-
334 G400RS, MGI Tech, Shenzhen, China) for cross-platform gene expression comparisons for
335 robust detection of EPO gene signatures. The studies were approved by the University of
336 Glasgow Ethics Committee (Scotland, UK) and the University of Brighton Ethics Committee
337 (England, UK) and were performed in accordance with the “Declaration of Helsinki”. Written
338 informed consent was obtained from all subjects.

339

340 **RNA collection and preparation**

341 Three milliliters of whole blood was collected from an antecubital vein using Tempus™
342 Blood RNA tubes (Thermo Fisher Scientific, Waltham, MA, USA). Each Tempus™ tube
343 contains 6 mL of RNA stabilising reagent and was vigorously mixed immediately after
344 collection for 10 s. The blood samples were incubated at room temperature for approximately 3
345 hours and then stored at -20°C or -80°C before subsequent analysis or transportation to the
346 analytical lab. Total RNA was isolated from the whole blood according to the manufacturer’s
347 instructions (Tempus™ Spin RNA Isolation Kit, Thermo Fisher Scientific, Waltham, MA,
348 USA). The purified total RNA was eluted in 90 μL elution buffer and stored in three aliquots at
349 -80°C until further analysis. Initial RNA quantity and purity was assessed by the Nanodrop™
350 ND-2000 Spectrophotometer (Thermo Fisher Scientific, Waltham, MA, US). RNA integrity was
351 assessed using the Agilent 2100 Bioanalyser (Agilent Technologies, Santa Clara, CA, USA)
352 prior to the RNA-seq and GeneChip analyses.

353

354 **Microarray analysis with HumanHT-12 v4.0 Expression BeadChip**

355 Detailed sample preparation for the Illumina microarray experiment are available elsewhere⁴.
356 Briefly, 500 ng of total RNA was used for complimentary RNA (cRNA) synthesis using the
357 IlluminaTM TotalPrep RNA Amplification Kit (Thermo Fisher Scientific, Waltham, MA, USA).
358 Seven hundred and fifty nanograms of the purified labelled cRNA samples were hybridised to
359 the HumanHT-12 v4.0 Expression BeadChip arrays containing > 47,000 probes, following the
360 manufacturer's recommended procedures (Illumina, San Diego, CA, USA). The Bead arrays
361 were scanned on the Illumina BeadArray Reader. In this current study, the raw intensity values
362 were exported using the Illumina GenomeStudio software (v2.0; Gene Expression Module). The
363 bioconductor "limma" package¹⁰ was used for background correction, data normalisation (using
364 the "neqc" function)²¹ and differential gene expression analysis (DGE)²² for paired samples
365 (using the "treat" function) in the 18 subjects across all 8 time points (i.e. Base1, Base2, EPO3,
366 EPO4, EPO5, Post6, Post7 and Post8). Notably, only probes expressed in at least 7 samples at a
367 detection $p < 0.05$ were kept. Probes were annotated to illuminaHumanv4.db²³ and only probes
368 with "good" and "perfect" matching quality were retained followed by removing probes with
369 "NA" or multiple mappings. Probes with low expression values below 5.1 were excluded prior
370 to the DGE analysis (assessed using the limma "plotSA" function). Transcripts were considered
371 significantly expressed for a fold change of 1.2 bounded to a 5% false discovery rate (FDR)
372 (thereby, giving more weight to fold change for gene ranking). These are common cut-off values
373 being used for declaring biologically and statistically significant findings in a DGE analysis²⁴.

374

375 **Microarray analysis with GeneChipTM HTA2.0**

376 One hundred nanograms of total RNA was processed using the GeneChipTM WT Plus Reagent
377 Kit according to the manufacturer's instructions (Thermo Fisher Scientific, Waltham, MA, US)

378 for 10 out of the 18 subjects at the selected time points (i.e. Base1, Base2, EPO3, EPO4 and
379 Post7). Single-stranded cDNA (ss-cDNA) was synthesised by the reverse transcription of cRNA.
380 Two hundred microlitres of hybridisation cocktail (containing approximately 5.2 µg fragmented
381 and labelled ss-cDNA) was loaded onto the GeneChip™ HTA2.0 (Thermo Fisher Scientific,
382 Waltham, MA, US). The GeneChip™ arrays were incubated in the GeneChip™ Hybridization
383 Oven 645 for 16 hours, washed and stained on the GeneChip™ Fluidics Station 450. The arrays
384 were then scanned using the GeneChip™ Scanner 3000 7G. The Applied Biosystems™
385 Transcriptome Analysis Console (version:4.0.1.36; Thermo Fisher Scientific, Waltham, MA,
386 US) was used to perform initial data QC and data visualisation. The relative log expression box
387 plots were plotted following the quality assessment steps illustrated in *ref*²⁵. The Bioconductor
388 “oligo” package²⁶ was used to read in the raw intensity CEL files, and the “rma” function was
389 used for background correction, normalisation, and data summarisation to the gene level (defined
390 by the argument “core”). Probes were annotated to hta20transcriptcluster.db²⁷ and probes with
391 “NA” or multiple mappings were removed. The “limma” package was then used to perform the
392 usual DGE analysis for paired samples (the analysis setting is identical to that used in the
393 Illumina microarray analysis illustrated above). Transcript clusters (loosely equal to genes) were
394 considered significantly expressed at a fold change of 1.2 bounded to a 5% FDR.

395

396 **RNA-seq on Illumina NextSeq500**

397 Five hundred nanograms of total RNA was used for sequencing according to the Illumina TruSeq
398 Stranded mRNA sample prep guide - high sample protocol (Illumina, San Diego, CA, USA).
399 Briefly, mRNA molecules were purified using the poly-T oligo attached magnetic beads
400 following which the mRNA was fragmented and primed for cDNA synthesis. A single “A” base

401 was subsequently added to the 3-prime end of the synthesised blunt-ended cDNA and ligated
402 with index adapters for hybridisation onto a flow cell. The DNA fragments with adapters on both
403 ends were amplified via polymerase chain reaction to generate the final double-stranded cDNA
404 (ds-cDNA) library followed by library validation and normalisation and pooling of the samples.
405 Samples were pooled and then sequenced at 2x75 bp read length to a depth of approximately 64
406 M reads per sample on the Illumina NextSeq 500 (Illumina, San Diego, CA, USA). 10 out of the
407 18 subjects at the selected time points (i.e. Base1, Base2, EPO3, EPO4, and Post7) were
408 analysed. Raw sequences were examined by FastQC²⁸ for basic quality checks (e.g. per base
409 sequence quality, adaptor content, and per base N content), FastQ Screen²⁹ for mapping against
410 multiple reference genomes for detecting sample swaps or sample contamination that may have
411 resulted from sources other than humans (i.e. in this case, mapping against human,
412 mouse and rat genomes were conducted), HISAT2⁵ for alignment to the reference genome
413 assembly (GRCh38.p12⁶) using the Ensembl 94 annotation³⁰ prior to RseQC⁷ for read
414 distribution analysis, Salmon⁸ for aligning to the transcriptome and transcripts quantification
415 (using selective alignment with the *decoy aware* target transcriptome to eliminate potential
416 spurious mapping to unannotated genomic locus over a *k*-mer length of 31, along with --SeqBias
417 and --gcBias flags switched on to correct for any unwanted effects), bioconductor package
418 “tximport”³¹ for summarising transcript-level estimates to genes based on Ensembl release 94³⁰,
419 and DESeq2⁹ for paired sample DGE analysis. Pre-filtering was performed to keep genes that
420 have at least 5 reads across 4 samples prior to the DGE analysis. Ensembl IDs were mapped to
421 gene symbols using the bioconductor package “org.Hs.eg.db”³² and un-defined mappings were
422 removed (i.e. gene with “NA” or multiple mappings). MultiQC³³ was used to aggregate the
423 analysis results from the FastQC, FastQ Screen and RseQC runs from multiple samples.

424 Unsupervised principal component analysis (PCA) for top 500 genes of high variance and gene
425 clustering analysis for the top 30 genes were performed following the DESeq2 vignette on data
426 quality assessment procedures³⁴. The bioconductor package “SVA”³⁵ was used to assess
427 surrogate variables that may represent other variations in the data for further correction.
428 Shrinkage estimator “apeglm” was used for the shrinkage of log fold change estimates and for
429 ranking genes by effect size³⁶. Genes exceeding a fold change of 1.2 bounded to the default *s*-
430 value < 0.005 were reported.

431

432 **RNA-seq on MGI DNBSEQ-G400RS**

433 Four hundred nanograms of total RNA was used for sequencing on the MGI DNBSEQ-G400RS
434 instrument (MGI, Shenzhen, China). Total RNA was first treated with Globin-Zero Gold Kit
435 (Illumina, San Diego, CA, USA) for rRNA depletion and globin mRNA reduction. The ds-
436 cDNA library preparation is in line with the Illumina RNA-seq protocol described in the above
437 section. The ds-cDNAs were then heat denatured and circularised by the splint oligo sequence to
438 generate the single strand circle DNA followed by rolling circle replication to create DNA
439 nanoballs (DNB) for processing on the MGI DNBSEQ-G400RS. The same 50 samples used for
440 the GeneChipTM and Illumina RNA-seq profiling were again analysed on this platform. These
441 samples were sequenced on 6 flowcells at 2x100 bp read length aimed at a sequencing depth of
442 64 M reads. Raw sequences were processed for quality assessment, alignment, transcripts
443 quantification and DGE analysis as described above in the “**RNA-seq on Illumina NextSeq500**”
444 section. The same cut-offs as in the Illumina RNA-seq section for defining a significant result
445 were applied (i.e. a fold change of 1.2 bounded to the default *s*-value < 0.005).

446

447 **Gene set enrichment analyses in GSEA and Reactome**

448 The pathway enrichment analysis was performed in accordance with recommendations from *ref*
449 ³⁷, where appropriate. Specifically, normalised RNA-seq counts (outputted from DESeq2
450 “counts” function with the argument “normalized=TRUE”) and normalised microarray gene
451 expression values were subjected to gene set enrichment analysis using GSEA (v4.0.3)^{11, 12} by
452 examining the Molecular Signatures Database (MSigDB)^{11, 13} Hallmark (H; containing 50 gene
453 sets)¹⁴ and Gene Ontology (C5; BP: subset of GO biological processes containing 7,573 gene
454 sets)^{15, 16} collections of functional gene sets. Low count genes (by removing genes with counts
455 below 5 in at least 4 samples) and genes with unidentified mappings from RNA-seq, and control
456 probes, low-quality probes and probes with unidentified mappings from microarray analyses
457 were excluded from the expression datasets prior to the GSEA. A standard GSEA run was
458 applied for each dataset by performing 1,000 phenotype permutations and by collapsing the
459 Ensembl IDs and probe IDs to gene symbols by mapping to their corresponding chip platforms
460 available from the MSigDB database (i.e. Human_ENSEMBL_Gene_ID_MSigDB.v7.2.chip for
461 RNA-seq, Human_AFFY_hta_2_0_MSigDB.v7.2.chip for GeneChipTM HTA2.0 and
462 Human_Illumina_HumanHT_12_v4_Array_MSigDB.v7.2.chip for Illumina BeadChip). Other
463 main parameters used in a GSEA run included the default ranking metric “Signal2Noise”, gene
464 set size filters (15-200 for H, and 10-500 for C5) and collapsing mode (“Sum_of_probes” for
465 RNA-seq, and “Max_probe” for microarray). Default values were used for other fields of the
466 GSEA run. EnrichmentMap App³⁸ was used for creating biological networks of the GSEA
467 pathways (pathway FDR<0.1, nominal P<0.05 and Jaccard Overlap coefficient >0.375 with
468 combined constant k=0.5) and AutoAnnotate App³⁹ for gene sets annotation and clustering
469 (MCL Cluster annotation) in Cytoscape (v3.8.0)⁴⁰. The most significantly enriched gene set was

470 used to label a gene set cluster, characterised by the normalised enrichment score (NES). Raw
471 counts from the RNA-seq (outputted from DESeq2 “counts” function by setting
472 “normalized=FALSE”), and normalised and log2 transformed gene expression values from
473 microarray analyses were uploaded onto Reactome (v73)²⁰ for quantitative pathway analysis
474 (ReactomeGSA) using the PADOG algorithm^{41, 42} for gene expression visualisation in pathway
475 diagrams. Protein-protein interactors derived from the IntAct database⁴³ with the IntAct score \geq
476 0.556 (of medium to high confidence interactions) were included in the analysis to improve the
477 Reactome pathway coverage. For consistency, these expression datasets were collapsed to gene
478 symbols using the “Collapse Dataset” tool in the GSEA software prior to the ReactomeGSA.

479

480 **Cross-platform DGE comparison**

481 Direct comparisons for the coding gene features identified across MGI DNBSEQ-G400RS,
482 Illumina NextSeq 500 and GeneChipTM HTA2.0 platforms in the 10 subjects (comprised of 50
483 samples) were carried out on the differentially expressed genes following the formal
484 DESeq2/limma DGE analyses. A sankey diagram was plotted for visualisation of the DGE
485 results using the “ggalluvial” package⁴⁴. The cross-platform correlations were computed using
486 the “ggscatter” function in the package “ggpubr”⁴⁵. “ggplot2”⁴⁶ and “cowplot”⁴⁷ packages were
487 used for creating publication-quality figures, where appropriate. Leading edge genes from the
488 significantly expressed GSEA pathways (derived from MGI DNBSEQ-G400RS, GeneChipTM
489 HTA2.0 and HumanHT-12 v4.0 Expression BeadChip; including all pathways with the NES>1.9
490 or the representative pathway of a gene set cluster when the NES<1.9) were extracted and
491 compared to the DGE genes to generate common sets of genes identified by both the GSEA and
492 DGE analyses. These genes were then overlapped with the DGE results obtained from the

493 Illumina NextSeq 500 platform for confirmation. The interaction networks among pathway genes
494 were defined by expression overlay with the Reactome pathway diagrams, focusing on the
495 networks represented by the confirmed genes above. The final lists of genes were obtained by
496 extracting all significantly altered genes and their interactors involved in these Reactome
497 networks and by matching them back to the differentially expressed genes resulted from the
498 formal DESeq2/limma analyses.

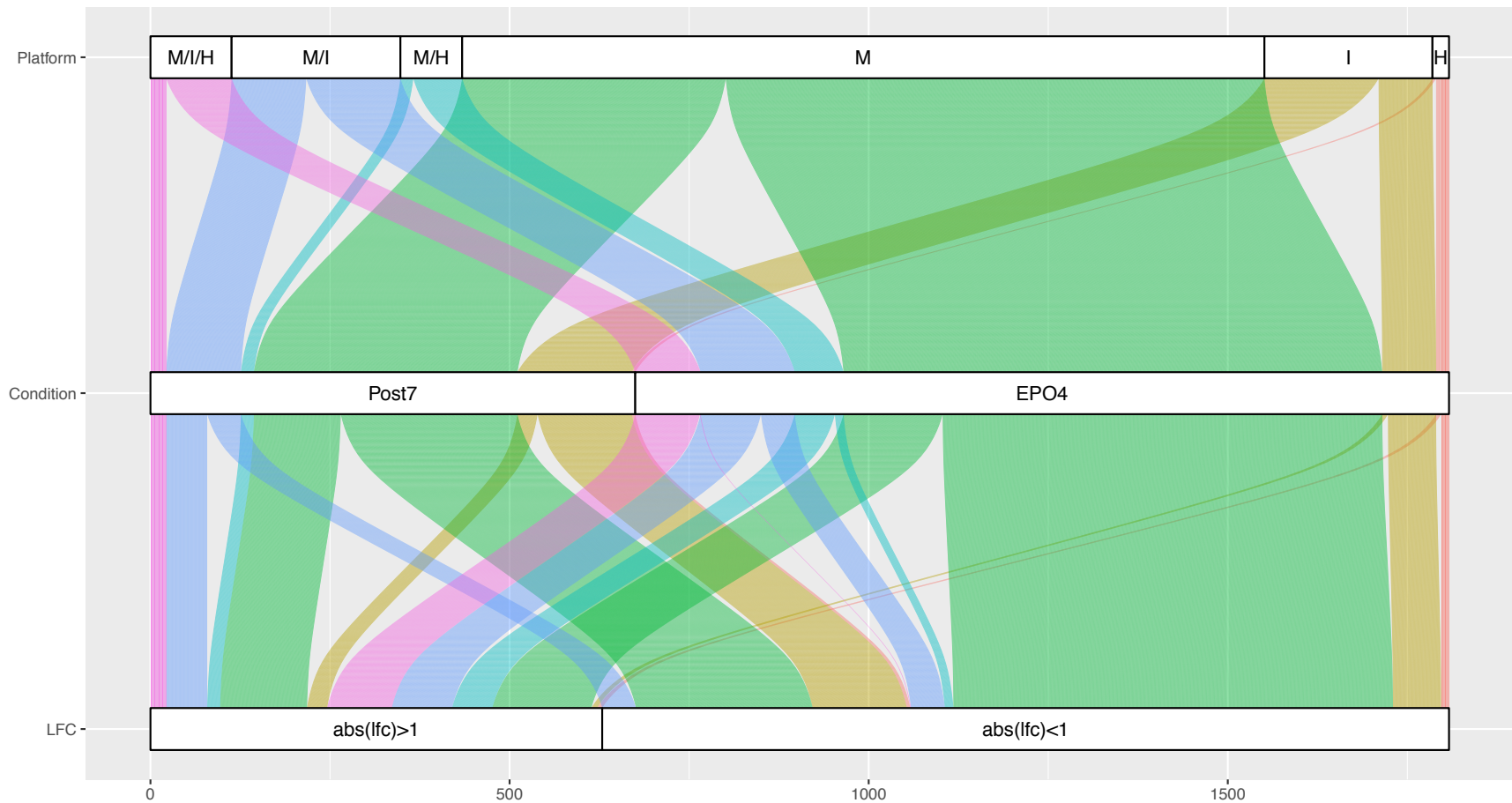
499

500 **Data availability:** Note all data will be made available and deposited into appropriate
501 repositories at publication, including raw RNA-seq data, raw microarray data, and code required
502 to reproduce all analyses. Full data access may be provided to reviewers on request during
503 manuscript reviewing.

504

505

506



507

508

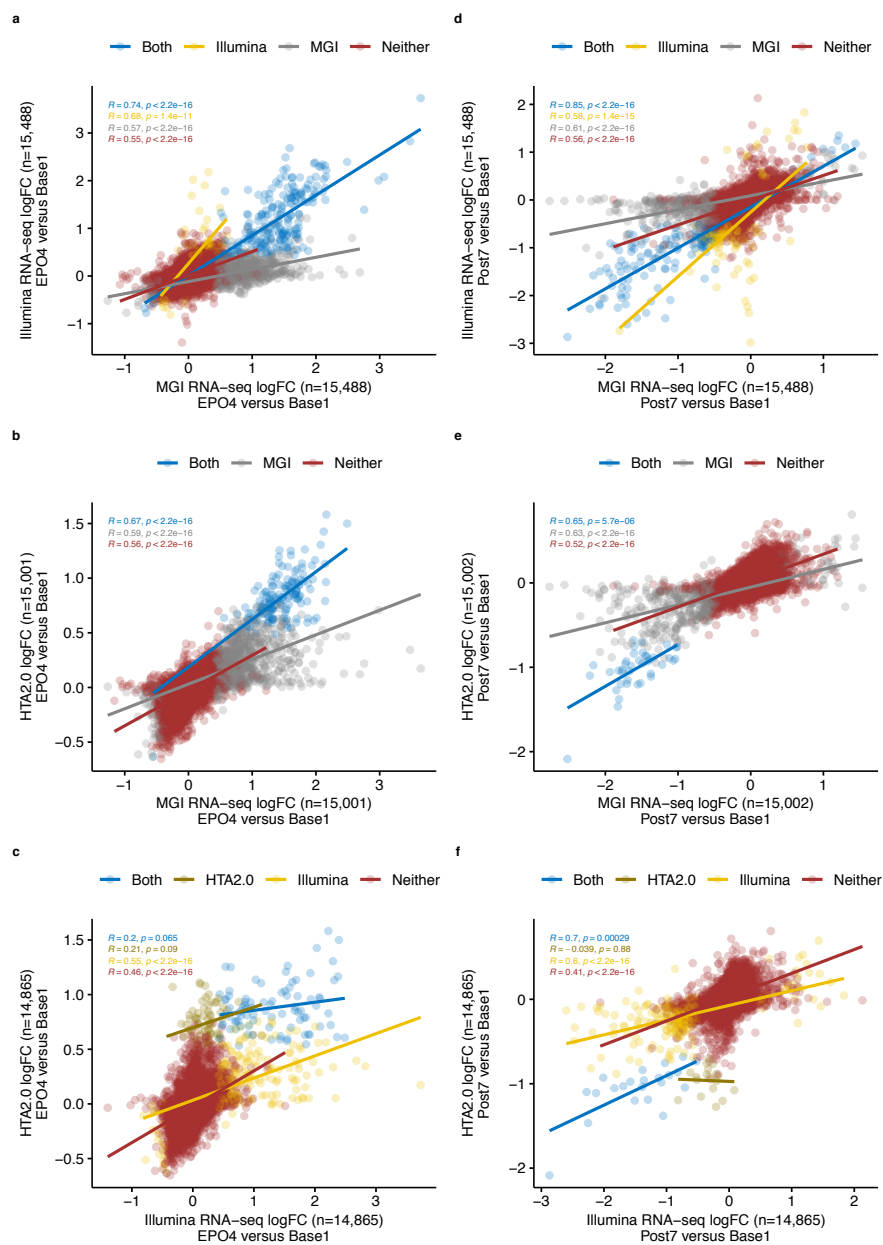
509

510

511

Fig. 1. Sankey diagram showing the flow of the differentially expressed gene features stratified by platform, biological condition and absolute log₂-transformed fold changes. M/I/H: MGI RNA-seq/Illumina RNA-seq/HTA2.0; M/I: MGI RNA-seq/Illumina RNA-seq; M/H: MGI RNA-seq/HTA2.0; M: MGI RNA-seq; I: Illumina RNA-seq; and H: HTA2.0. abs(lfc): absolute log₂-transformed fold change. The colour coded band represents a detection platform or a combination of the detection platforms. The

512 wider the band, the higher number of the identified features on a platform or across platforms. The x-axis represents the number of
513 identified features captured on each platform. Note, for M/I/H, M/I, and M/H, that biological magnitude of the features used for
514 stratification is based on the MGI RNA-seq DGE results. Thirty-four identified non-protein coding transcript clusters on the GeneChip
515 are removed for the purposes of cross-platform comparison.

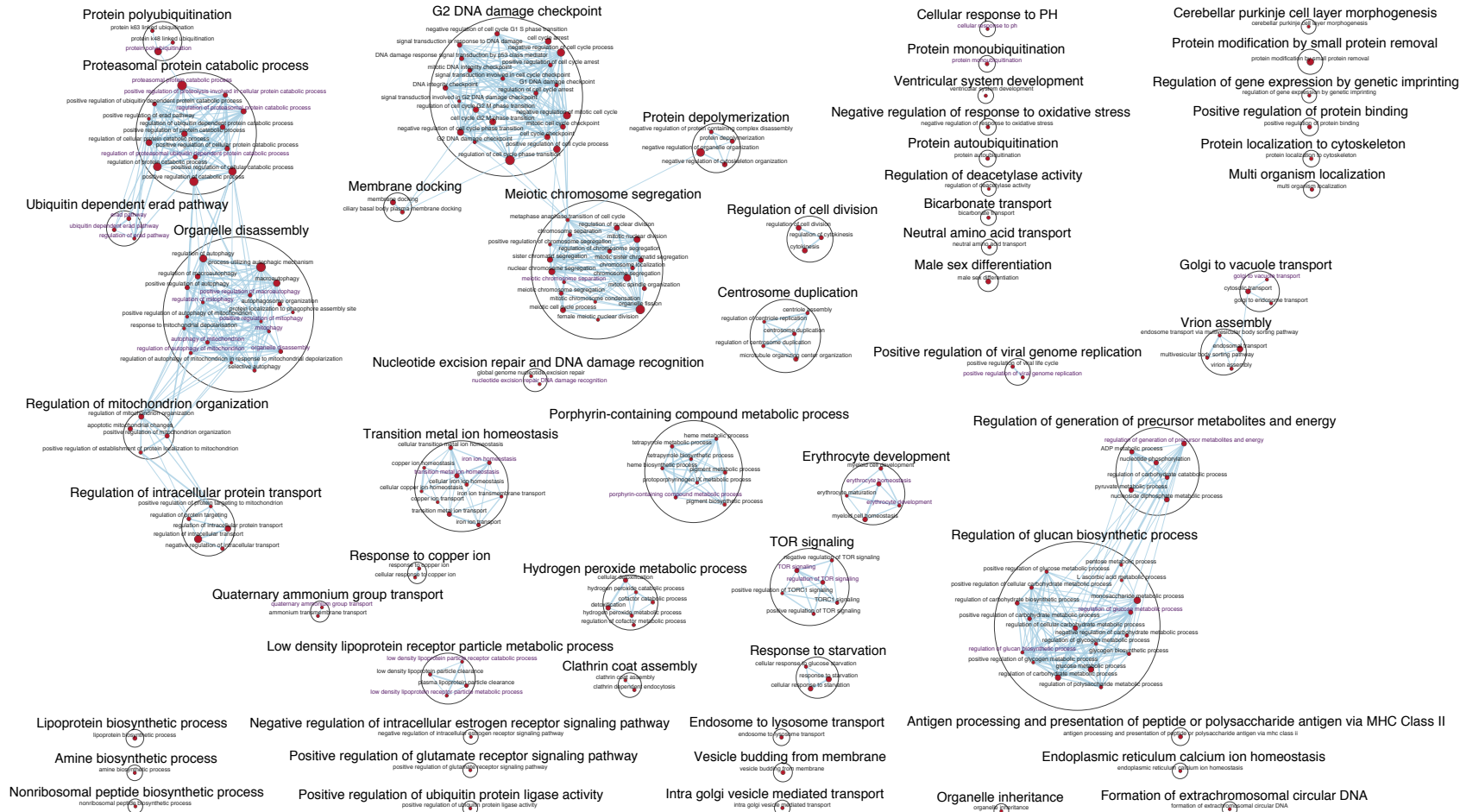


517

518 **Fig. 2. Cross-platform gene expression correlation analyses of log₂-transformed fold**
 519 **changes of all identified gene features. a-c** Genes identified when compared the level of
 520 expression between EPO4 and Base1 among the platform pairs in Illumina-MGI RNA-seq (a),
 521 GeneChip™ HTA2.0-MGI RNA-seq (b), GeneChip™ HTA2.0-Illumina RNA-seq (c). **d-f**
 522 Genes identified when compared the level of expression between Post7 and Base1 among the

523 platform pairs in Illumina-MGI RNA-seq (**d**), GeneChipTM HTA2.0-MGI RNA-seq (**e**),
524 GeneChipTM HTA2.0-Illumina RNA-seq (**f**). Genes identified as differentially expressed by
525 each pair are plotted in blue; genes that are only differentially expressed in Illumina RNA-seq,
526 MGI RNA-seq or GeneChipTM HTA2.0 are plotted in yellow, grey and dijon, respectively; genes
527 not identified as differentially expressed by a pair are plotted in red. For simplicity, the
528 maximum expression value of a gene was used when multiple mapping of transcripts to the same
529 gene occurred. *FOXO3B* is only differentially expressed in GeneChipTM HTA2.0 when
530 compared to the MGI RNA-seq findings in (**b**), thus it has been removed from the correlation
531 analysis. R: Pearson's r . LogFC: \log_2 -transformed fold change.

532
533



534

535

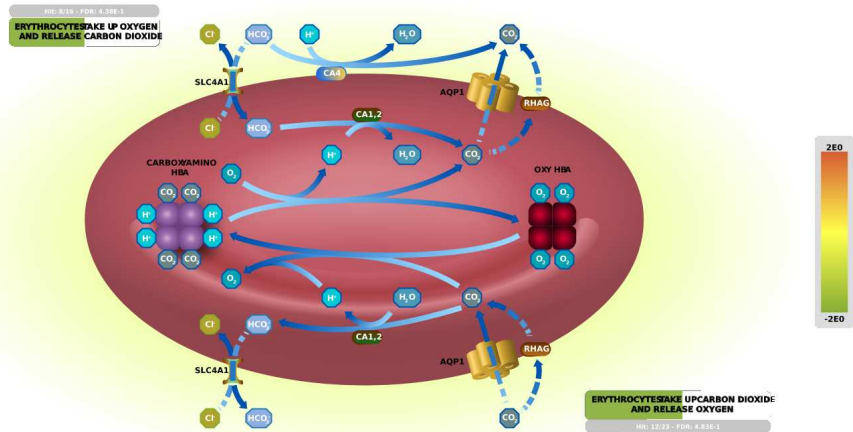
536

Fig. 3. Biological network of the MGI RNA-seq dataset following Gene Ontology (biological process) gene set enrichment analysis in GSEA (v4.0.3) and visualisation in Cytoscape (3.8.0). Each circle (node) represents a gene set and two nodes are

537 connected by lines (edges) indicating shared genes. The size of a node and width of an edge are proportional to the number of genes
538 enriched in a gene set and the number of genes shared between gene sets, respectively. Gene sets that are similar were annotated and
539 clustered to form a biological theme using the AutoAnnotate App in Cytoscape. The most significantly enriched gene set is used to
540 label a gene set cluster, defined by NES. Red node: gene set enriched in EPO4. Purple node label: top gene sets with NES > 1.90. The
541 enrichment map was created with pathway FDR < 0.1, nominal $P < 0.05$ and Jaccard Overlap coefficient > 0.375 with combined
542 constant $k = 0.5$.

543

544



545

546

547

548

549

550

551

552

553

554

Fig. 4. Enhanced high-level Reactome pathway diagram for O₂/CO₂ exchange in erythrocytes⁴⁸ by expression overlay with the MGI RNA-seq Post7 dataset. This high-level diagram represents two subpathways, namely erythrocyte take up oxygen and release carbon dioxide and erythrocyte take up carbon dioxide and release oxygen. The green band indicates the proportion of the pathway that is represented in the MGI RNA-seq Post7 dataset, and the colour (green) represents the down-regulation of the pathway genes. The grey bar contains the information for the number of pathway entities in the query dataset, the total number of the pathway entities, and the FDR corrected over-representation probability.

555
556
557
558
559
560
561
562
563
564
565
566
567
568
569
570
571
572
573
574
575
576
577

References:

1. Shendure, J. et al., DNA sequencing at 40: past, present and future. *Nature*. **550**, 345-353 (2017).
2. Manolio, T. A. et al., Genomic Medicine Year in Review: 2019. *Am. J. Hum. Genet.* **105**, 1072-1075 (2019).
3. Durussel, J. et al., Haemoglobin mass and running time trial performance after recombinant human erythropoietin administration in trained men. *PLoS One*. **8**, e56151 (2013).
4. Durussel, J. et al., Blood transcriptional signature of recombinant human erythropoietin administration and implications for antidoping strategies. *Physiol. Genomics*. **48**, 202-209 (2016).
5. Kim, D., Paggi, J. M., Park, C., Bennett, C., Salzberg, S. L., Graph-based genome alignment and genotyping with HISAT2 and HISAT-genotype. *Nat. Biotechnol.* **37**, 907-915 (2019).
6. Schneider, V. A. et al., Evaluation of GRCh38 and de novo haploid genome assemblies demonstrates the enduring quality of the reference assembly. *Genome Res.* **27**, 849-864 (2017).
7. Wang, L., Wang, S., Li, W., RSeQC: quality control of RNA-seq experiments. *Bioinformatics*. **28**, 2184-2185 (2012).
8. Patro, R., Duggal, G., Love, M. I., Irizarry, R. A., Kingsford, C., Salmon provides fast and bias-aware quantification of transcript expression. *Nat. Methods*. **14**, 417-419 (2017).
9. Love, M. I., Huber, W., Anders, S., Moderated estimation of fold change and dispersion for RNA-seq data with DESeq2. *Genome Biol.* **15**, 550 (2014).
10. Ritchie, M. E. et al., limma powers differential expression analyses for RNA-sequencing and microarray studies. *Nucleic Acids Res.* **43**, e47 (2015).

- 578 11. Subramanian, A. et al., Gene set enrichment analysis: a knowledge-based approach for
579 interpreting genome-wide expression profiles. *Proc. Natl. Acad. Sci. U. S. A.* **102**, 15545-15550
580 (2005).
- 581 12. Mootha, V. K. et al., PGC-1alpha-responsive genes involved in oxidative phosphorylation
582 are coordinately downregulated in human diabetes. *Nat. Genet.* **34**, 267-273 (2003).
- 583 13. Liberzon, A. et al., Molecular signatures database (MSigDB) 3.0. *Bioinformatics.* **27**, 1739-
584 1740 (2011).
- 585 14. Liberzon, A. et al., The Molecular Signatures Database (MSigDB) hallmark gene set
586 collection. *Cell Syst.* **1**, 417-425 (2015).
- 587 15. Ashburner, M. et al., Gene ontology: tool for the unification of biology. The Gene Ontology
588 Consortium. *Nat. Genet.* **25**, 25-29 (2000).
- 589 16. The Gene Ontology Consortium. The Gene Ontology Resource: 20 years and still GOing
590 strong. *Nucleic Acids Res.* **47**, D330-d338 (2019).
- 591 17. Ghezzi, P., Brines, M., Erythropoietin as an antiapoptotic, tissue-protective cytokine. *Cell*
592 *Death Differ.* **11 Suppl 1**, S37-44 (2004).
- 593 18. Jelkmann, W., Regulation of erythropoietin production. *J. Physiol.* **589**, 1251-1258 (2011).
- 594 19. Maiese, K., Erythropoietin and diabetes mellitus. *World J. Diabetes.* **6**, 1259-1273 (2015).
- 595 20. Jassal, B. et al., The reactome pathway knowledgebase. *Nucleic Acids Res.* **48**, D498-d503
596 (2020).
- 597 21. Shi, W., Oshlack, A., Smyth, G. K., Optimizing the noise versus bias trade-off for Illumina
598 whole genome expression BeadChips. *Nucleic Acids Res.* **38**, e204 (2010).

- 599 22. Phipson, B., Lee, S., Majewski, I. J., Alexander, W. S., Smyth, G. K., Robust hyperparameter
600 estimation protects against hypervariable genes and improves power to detect differential
601 expression. *Ann. Appl. Stat.* **10**, 946-963 (2016).
- 602 23. Dunning, M., Lynch, A., Eldridge, M., illuminaHumanv4.db: Illumina HumanHT12v4
603 annotation data (chip illuminaHumanv4). R package version 1.26.0. (2015).
- 604 24. Vaes, E., Khan, M., Mombaerts, P., Statistical analysis of differential gene expression
605 relative to a fold change threshold on NanoString data of mouse odorant receptor genes. *BMC*
606 *Bioinformatics.* **15**, 39 (2014).
- 607 25. Klaus, B., Reisenauer, S., An end to end workflow for differential gene expression using
608 Affymetrix microarrays. *F1000Res.* **5**, 1384 (2016).
- 609 26. Carvalho, B. S., Irizarry, R. A., A framework for oligonucleotide microarray preprocessing.
610 *Bioinformatics.* **26**, 2363-2367 (2010).
- 611 27. MacDonald, J. W., hta20transcriptcluster.db: Affymetrix hta20 annotation data (chip
612 hta20transcriptcluster). R package version 8.7.0. (2017).
- 613 28. Andrews, S., FastQC: A Quality Control Tool for High Throughput Sequence Data [Online].
614 Available online at: <http://www.bioinformatics.babraham.ac.uk/projects/fastqc/>. (2010).
- 615 29. Wingett, S. W., Andrews, S., FastQ Screen: A tool for multi-genome mapping and quality
616 control. *F1000Res.* **7**, 1338 (2018).
- 617 30. Ensembl Archive Release 94 (October 2018). Available at:
618 <http://oct2018.archive.ensembl.org/index.html>. (2018).
- 619 31. Sonesson, C., Love, M. I., Robinson, M. D., Differential analyses for RNA-seq: transcript-
620 level estimates improve gene-level inferences. *F1000Res.* **4**, 1521 (2015).

621 32. Carlson, M., org.Hs.eg.db: Genome wide annotation for Human. R package version 3.8.2.,
622 (2019).

623 33. Ewels, P., Magnusson, M., Lundin, S., Källner, M., MultiQC: summarize analysis results for
624 multiple tools and samples in a single report. *Bioinformatics*. **32**, 3047-3048 (2016).

625 34. Love, M. I., Anders, S., Huber, W., Analyzing RNA-seq data with DESeq2. Available at:
626 <https://www.bioconductor.org/packages/devel/bioc/vignettes/DESeq2/inst/doc/DESeq2.html> -
627 [references](#). (2020).

628 35. Leek, J. T. et al., sva: Surrogate Variable Analysis. R package version 3.38.0. (2020).

629 36. Zhu, A., Ibrahim, J. G., Love, M. I., Heavy-tailed prior distributions for sequence count data:
630 removing the noise and preserving large differences. *Bioinformatics*. **35**, 2084-2092 (2019).

631 37. Reimand, J. et al., Pathway enrichment analysis and visualization of omics data using
632 g:Profiler, GSEA, Cytoscape and EnrichmentMap. *Nat. Protoc.* **14**, 482-517 (2019).

633 38. Merico, D., Isserlin, R., Stueker, O., Emili, A., Bader, G. D., Enrichment map: a network-
634 based method for gene-set enrichment visualization and interpretation. *PLoS One*. **5**, e13984
635 (2010).

636 39. Kucera, M., Isserlin, R., Arkhangorodsky, A., Bader, G. D., AutoAnnotate: A Cytoscape app
637 for summarizing networks with semantic annotations. *FI000Res*. **5**, 1717 (2016).

638 40. Shannon, P. et al., Cytoscape: a software environment for integrated models of biomolecular
639 interaction networks. *Genome Res*. **13**, 2498-2504 (2003).

640 41. Tarca, A. L., Draghici, S., Bhatti, G., Romero, R., Down-weighting overlapping genes
641 improves gene set analysis. *BMC Bioinformatics*. **13**, 136 (2012).

642 42. Griss, J. et al., ReactomeGSA - Efficient Multi-Omics Comparative Pathway Analysis. *Mol.*
643 *Cell. Proteomics*. (2020).

644 43. Orchard, S. et al., The MIntAct project--IntAct as a common curation platform for 11
645 molecular interaction databases. *Nucleic Acids Res.* **42**, D358-363 (2014).

646 44. Brunson, J. C., ggalluvial: Layered Grammar for Alluvial Plots. *J. Open Source Softw.* **5**, 49
647 (2017).

648 45. Kassambara, A., ggpubr: 'ggplot2' based publication ready plots. R package version 0.4.0.
649 (2020).

650 46. Wickham, H., *Elegant graphics for data analysis*. Springer-Verlag New York. (2016).

651 47. Wilke, C. O., cowplot: streamlined plot theme and plot annotations for 'ggplot2'. R package
652 version 1.1.1. (2020).

653 48. O2/CO2 exchange in erythrocytes. Reactome, released 2012-06-12,
654 doi:10.3180/REACT_120969.1 (11/11/20).

655

656 **Acknowledgments:**

657 We thank BGI Hong Kong for conducting the DNB-seq. This work was funded by the World
658 Anti-Doping Agency (WADA) grant no. 08C19YP and ISF15E10YP to YPP. GIA was
659 supported by a fellowship from the Office of Academic Affiliations at the United States Veterans
660 Health Administration.

661 **Author contributions:**

662 Conceptualization: GW, YPP; Formal analysis: GW; Funding acquisition: YPP; Investigation:
663 GW, TK; Methodology: GW, YPP; Project administration: AC, QM; Resources: GIA, JL, MBG;
664 Supervision: YPP; Validation: GW; Visualization: GW; Writing – original draft: GW; Writing –
665 review & editing: AH, FMG, GIA, JL, MBG, YPP, GW.

666 **Competing interests:**

667 The authors declare no competing interests.

668 **Materials & Correspondence:**

669 Correspondence and material requests should be addressed to GW and YPP.

670

671

672 **Figure legends:**

673

674

675

Fig. 1. Sankey diagram ⁴⁴ showing the flow of the differentially expressed gene features stratified by platform, biological condition and absolute log₂-transformed fold changes.

676

677

M/I/H: MGI RNA-seq/Illumina RNA-seq/HTA2.0; M/I: MGI RNA-seq/Illumina RNA-seq;

678

M/H: MGI RNA-seq/HTA2.0; M: MGI RNA-seq; I: Illumina RNA-seq; and H: HTA2.0.

679

abs(lfc): absolute log₂-transformed fold change. The colour coded band represents a detection

680

platform or a combination of the detection platforms. The wider the band, the higher number of

681

the identified features on a platform or across platforms. The x-axis represents the number of

682

identified features captured on each platform. Note, for M/I/H, M/I, and M/H, that biological

683

magnitude of the features used for stratification is based on the MGI RNA-seq DGE results.

684

Thirty-four identified non-protein coding transcript clusters on the GeneChip are removed for the

685

purposes of cross-platform comparison.

686

Fig. 2. Cross-platform gene expression correlation analyses of log₂-transformed fold

687

changes of all identified gene features. a-c Genes identified when compared the level of

688

expression between EPO4 and Base1 among the platform pairs in Illumina-MGI RNA-seq (**a**),

689

GeneChipTM HTA2.0-MGI RNA-seq (**b**), GeneChipTM HTA2.0-Illumina RNA-seq (**c**). **d-f**

690

Genes identified when compared the level of expression between Post7 and Base1 among the

691

platform pairs in Illumina-MGI RNA-seq (**d**), GeneChipTM HTA2.0-MGI RNA-seq (**e**),

692

GeneChipTM HTA2.0-Illumina RNA-seq (**f**). Genes identified as differentially expressed by

693

each pair are plotted in blue; genes that are only differentially expressed in Illumina RNA-seq,

694

MGI RNA-seq or GeneChipTM HTA2.0 are plotted in yellow, grey and dijon, respectively; genes

695

not identified as differentially expressed by a pair are plotted in red. For simplicity, the

696

maximum expression value of a gene was used when multiple mapping of transcripts to the same

697 gene occurred. FOXO3B is only differentially expressed in GeneChip™ HTA2.0 when
698 compared to the MGI RNA-seq findings in (b), thus it has been removed from the correlation
699 analysis. R: Pearson's r. LogFC: log₂-transformed fold change.

700 **Fig. 3. Biological network of the MGI RNA-seq dataset following Gene Ontology (biological**
701 **process) gene set enrichment analysis in GSEA (v4.0.3) and visualisation in Cytoscape**
702 **(3.8.0)**⁴⁰. Each circle (node) represents a gene set and two nodes are connected by lines (edges)
703 indicating shared genes. The size of a node and width of an edge are proportional to the number
704 of genes enriched in a gene set and the number of genes shared between gene sets, respectively.
705 Gene sets that are similar were annotated and clustered to form a biological theme using the
706 AutoAnnotate App³⁹ in Cytoscape. The most significantly enriched gene set is used to label a
707 gene set cluster, defined by NES. Red node: gene set enriched in EPO4. Purple node label: top
708 gene sets with NES > 1.90. The enrichment map was created with pathway FDR < 0.1, nominal
709 $P < 0.05$ and Jaccard Overlap coefficient > 0.375 with combined constant $k = 0.5$.

710 **Fig. 4. Enhanced high-level Reactome pathway diagram for O₂/CO₂ exchange in**
711 **erythrocytes**⁴⁸ **by expression overlay with the MGI RNA-seq Post7 dataset.** This high-level
712 diagram represents two subpathways, namely erythrocyte take up oxygen and release carbon
713 dioxide and erythrocyte take up carbon dioxide and release oxygen. The green band indicates the
714 proportion of the pathway that is represented in the MGI RNA-seq Post7 dataset, and the colour
715 (green) represents the down-regulation of the pathway genes. The grey bar contains the
716 information for the number of pathway entities in the query dataset, the total number of the
717 pathway entities, and the FDR corrected over-representation probability.

718
719

720 **Table 1.** Summary of the number of transcriptomic features available for the DGE analysis
 721 across the four gene expression detection platforms.

722

	MGI DNBSEQ- G400RS	Illumina NextSeq 500	GeneChip™ HTA2.0	Illumina HumanHT-12 v4 Expression BeadChip
Number of samples	50	48	49	143
Number of transcriptomic features following RNA-seq quantification (Salmon) or on the array	175,775	175,775	285,543	47,286
Number of identified features available for the DGE analysis	16,738 ^g	16,581 ^g	29,517 ^{tc}	10,622 ^t

723

724

725

726

727

728

DGE: differential gene expression. g: protein-coding gene features. tc: protein coding and non-protein coding transcript clusters, loosely corresponding to genes. t: coding and non-coding transcripts. Two, one and one samples were removed from the DGE analyses due to human processing errors, sample quality and sampling issue in the Illumina RNA-seq, GeneChip and BeadChip datasets, respectively.

Table 2. Transcript annotation and filtering of the RNA-seq and microarray data prior to the DGE analysis.

	MGI DNBSEQ-G400RS	Illumina NextSeq 500	GeneChip™ HTA2.0	Illumina HumanHT- 12 v4 Expression BeadChip
Annotation database (N=the number of transcriptomic features)	Org.Hs.eg.db (N=175,775 transcripts following Salmon transcription quantification, aggregated into 37,788 genes using Ensembl 94 annotation)	Org.Hs.eg.db (N=175,775 transcripts following Salmon transcription quantification, aggregated into 37,788 genes using Ensembl 94 annotation)	hta20transcriptcluster.db (N=285,543 transcripts, corresponding to 67,480 protein-coding and non-protein coding transcript clusters)	illuminaHumanv4.db (N=47,286 coding and non-coding transcripts)
Undetected probes	-	-	-	18,494
Low quality probes	-	-	-	6,900
Low-expressed genes (RNA-seq)	17,198	18,347	-	-
“NA” mapping to stable gene symbols	3,675	2,668	36,709	2,406
Multiple mapping to stable gene symbols	177	192	1,254	698
Low-expressed probes (microarray) ¹	-	-	0	8,166
Identified features available for DGE analysis	16,738 ^g	16,581 ^g	29,517 ^{tc}	10,622 ^t

730

731

732

NA: features with no gene symbols returned after annotation. DGE: differential gene expression. -: not applicable. ¹: low expressed probes were further removed following assessing the average log expression and the mean-variance relationship after fitting the linear

733 model in limma microarray analysis. g: protein-coding gene features. tc: protein-coding and non-protein coding transcript clusters,
734 loosely corresponding to genes. t: coding and non-coding transcript features.

735

Table 3. Summary of the number of significantly expressed transcriptomic features across all platforms.

736

	DGE thresholds	Base2 vs Base1	EPO3 vs Base1	EPO4 vs Base1	Post7 vs Base1	Up/down regulation
MGI DNBSEQ-G400RS (N = 50)	abs FC > 1.2 & s-value < 0.005	0	1	959	60	Up
		0	0	81	451	Down
Illumina NextSeq 500 (N = 48)	abs FC > 1.2 & s-value < 0.005	0	0	277	27	Up
		0	0	20	258	Down
GeneChip™ HTA2.0 (N = 49)	abs FC > 1.2 & FDR < 0.05	0	0	200	0	Up
		0	0	1	51	Down
Illumina HumanHT-12v4.0 Expression Beadchip (N = 143)	abs FC > 1.2 & FDR < 0.05	0	13	796	7	Up
		0	0	1,315	254	Down

737

738

739

740

741

DGE: differential gene expression. abs FC: absolute fold change. FDR: false discovery rate. The number of protein-coding gene features, and coding and non-coding transcript clusters and transcripts are reported following the RNA-seq, GeneChip and Beadchip DGE analyses, respectively.

Figures

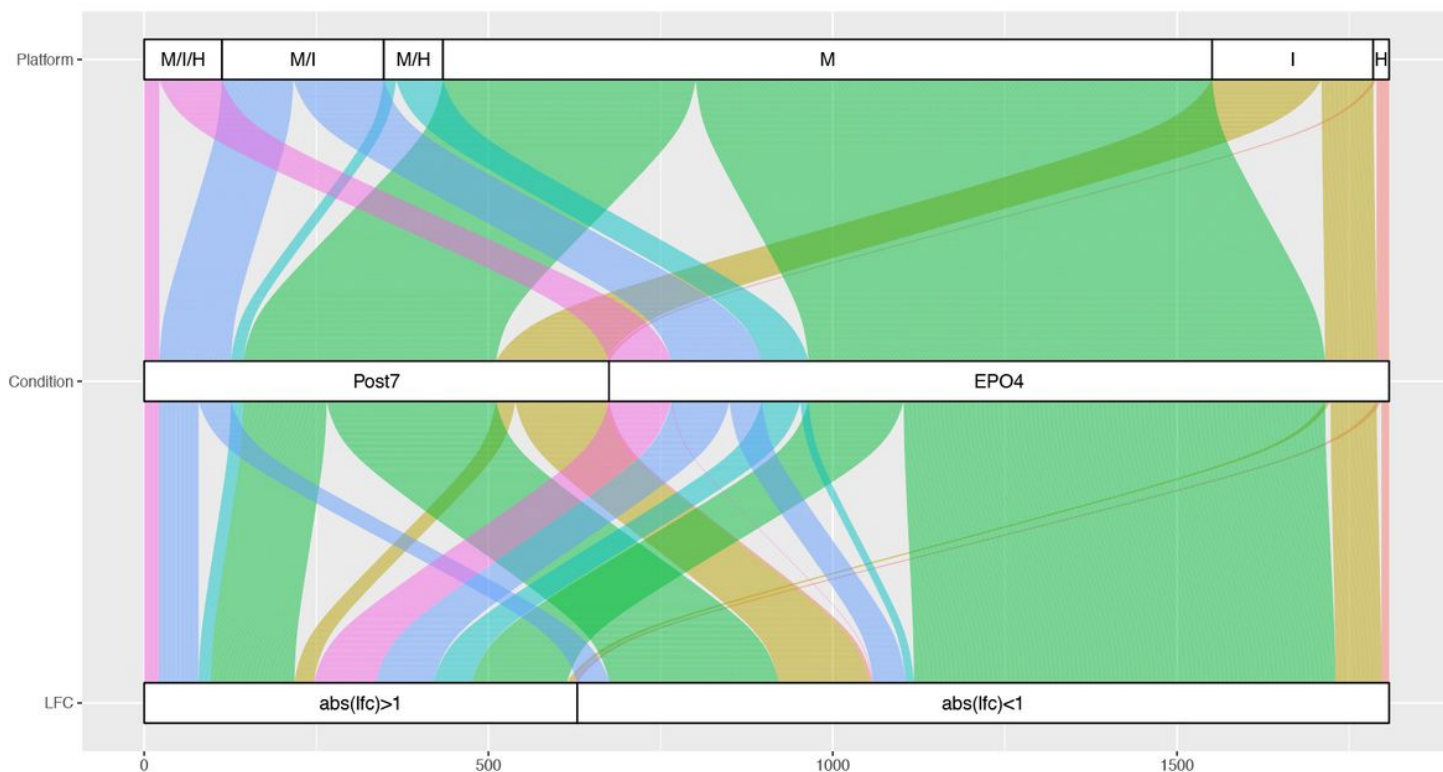


Figure 1

Sankey diagram 44 showing the flow of the differentially expressed gene features stratified by platform, biological condition and absolute log₂-transformed fold changes. M/I/H: MGI RNA-seq/Illumina RNA-seq/HTA2.0; M/I: MGI RNA-seq/Illumina RNA-seq; M/H: MGI RNA-seq/HTA2.0; M: MGI RNA-seq; I: Illumina RNA-seq; and H: HTA2.0. $abs(lfc)$: absolute log₂-transformed fold change. The colour coded band represents a detection platform or a combination of the detection platforms. The wider the band, the higher number of the identified features on a platform or across platforms. The x-axis represents the number of identified features captured on each platform. Note, for M/I/H, M/I, and M/H, that biological magnitude of the features used for stratification is based on the MGI RNA-seq DGE results. Thirty-four identified non-protein coding transcript clusters on the GeneChip are removed for the purposes of cross-platform comparison.

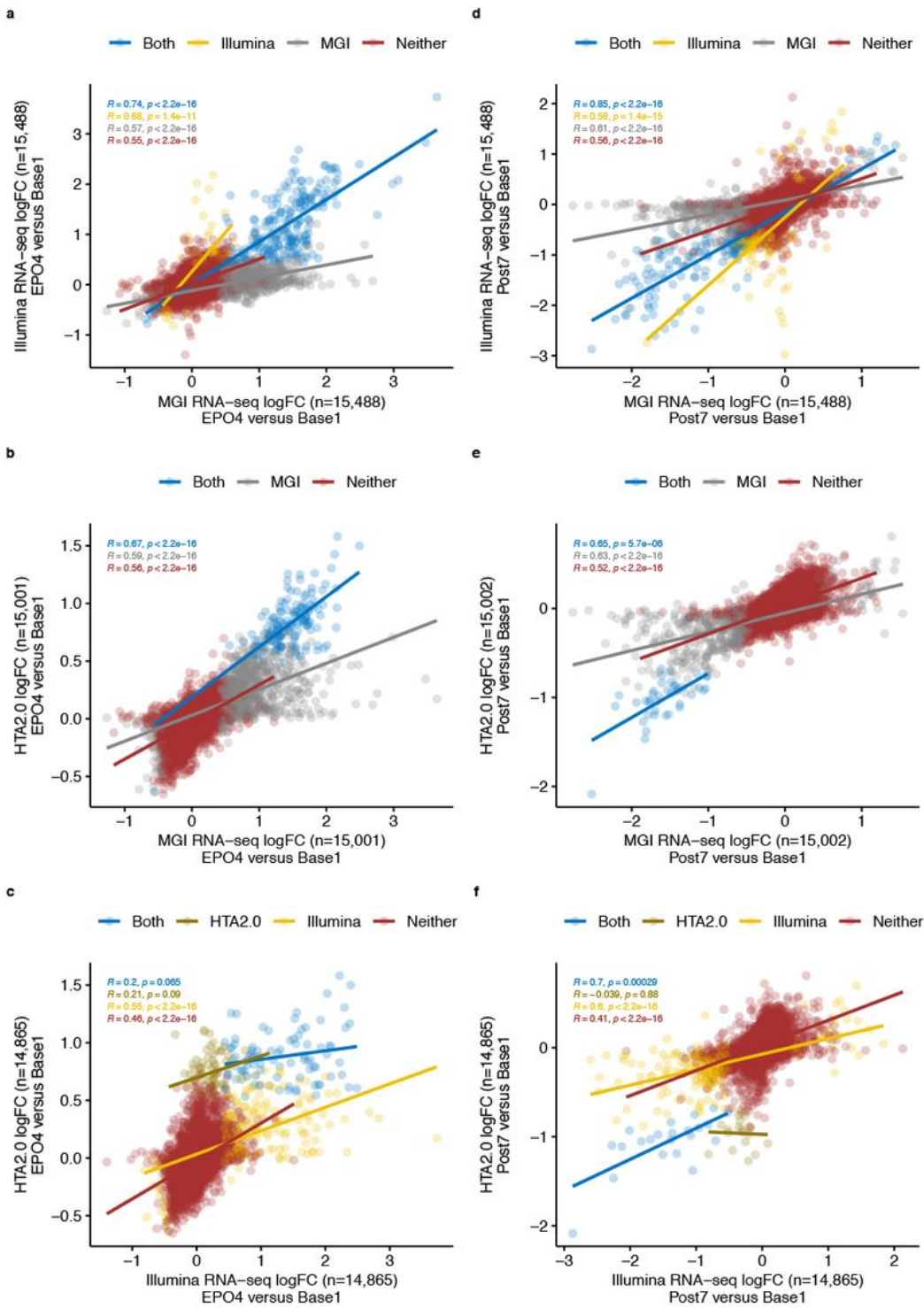


Figure 2

Cross-platform gene expression correlation analyses of log₂-transformed fold changes of all identified gene features. a-c Genes identified when compared the level of expression between EPO4 and Base1 among the platform pairs in Illumina-MGI RNA-seq (a), GeneChip™ HTA2.0-MGI RNA-seq (b), GeneChip™ HTA2.0-Illumina RNA-seq (c). d-f Genes identified when compared the level of expression between Post7 and Base1 among the platform pairs in Illumina-MGI RNA-seq (d), GeneChip™ HTA2.0-

MGI RNA-seq (e), GeneChipTM HTA2.0-Illumina RNA-seq (f). Genes identified as differentially expressed by each pair are plotted in blue; genes that are only differentially expressed in Illumina RNA-seq, MGI RNA-seq or GeneChipTM HTA2.0 are plotted in yellow, grey and dijon, respectively; genes not identified as differentially expressed by a pair are plotted in red. For simplicity, the maximum expression value of a gene was used when multiple mapping of transcripts to the same gene occurred. FOXO3B is only differentially expressed in GeneChipTM HTA2.0 when compared to the MGI RNA-seq findings in (b), thus it has been removed from the correlation analysis. R: Pearson's r. LogFC: log2-transformed fold change.

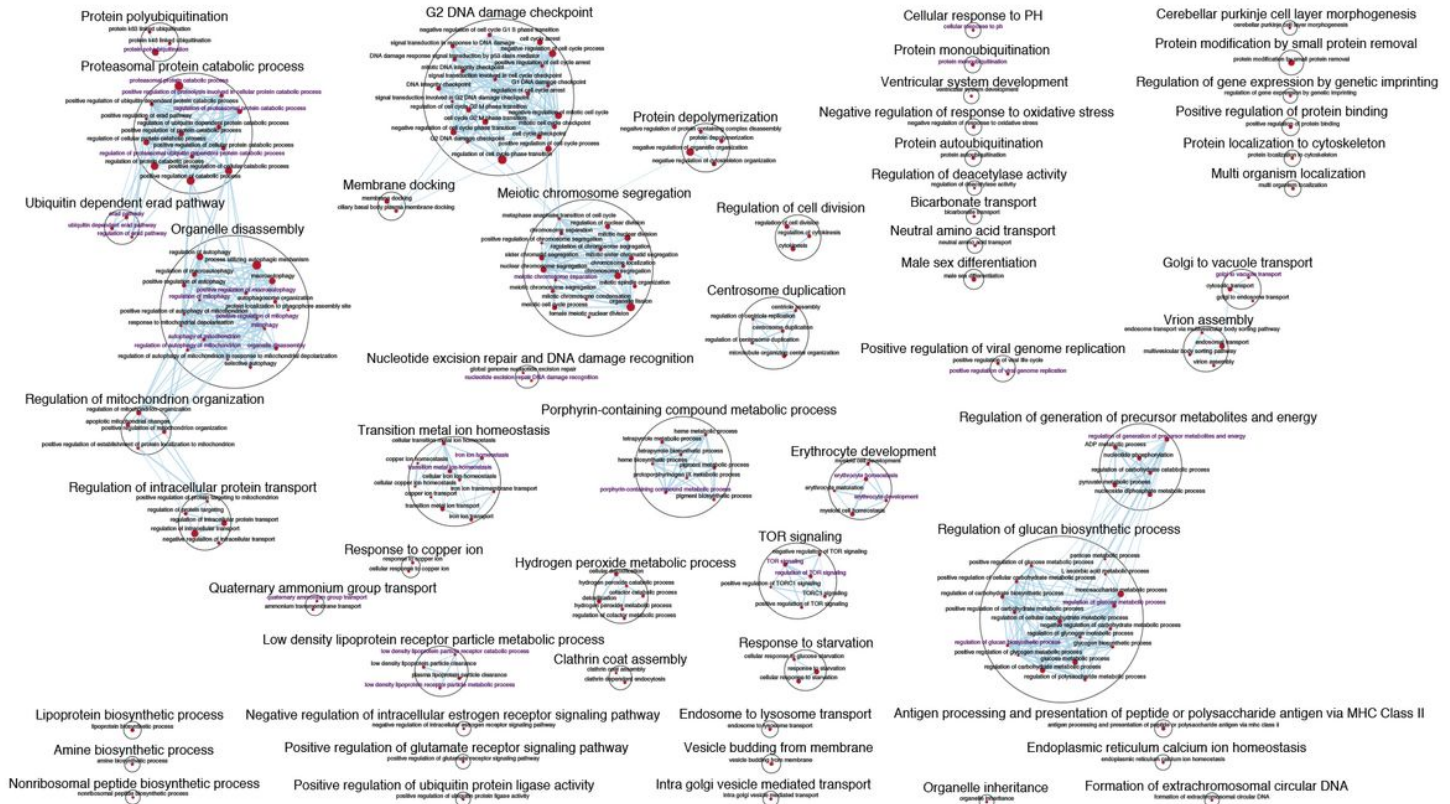


Figure 3

Biological network of the MGI RNA-seq dataset following Gene Ontology (biological process) gene set enrichment analysis in GSEA (v4.0.3) and visualisation in Cytoscape (3.8.0) 40. Each circle (node) represents a gene set and two nodes are connected by lines (edges) indicating shared genes. The size of a node and width of an edge are proportional to the number of genes enriched in a gene set and the number of genes shared between gene sets, respectively. Gene sets that are similar were annotated and clustered to form a biological theme using the AutoAnnotate App 39 in Cytoscape. The most significantly enriched gene set is used to label a gene set cluster, defined by NES. Red node: gene set enriched in EPO4. Purple node label: top gene sets with NES > 1.90. The enrichment map was created with pathway FDR < 0.1, nominal P < 0.05 and Jaccard Overlap coefficient > 0.375 with combined constant k = 0.5.

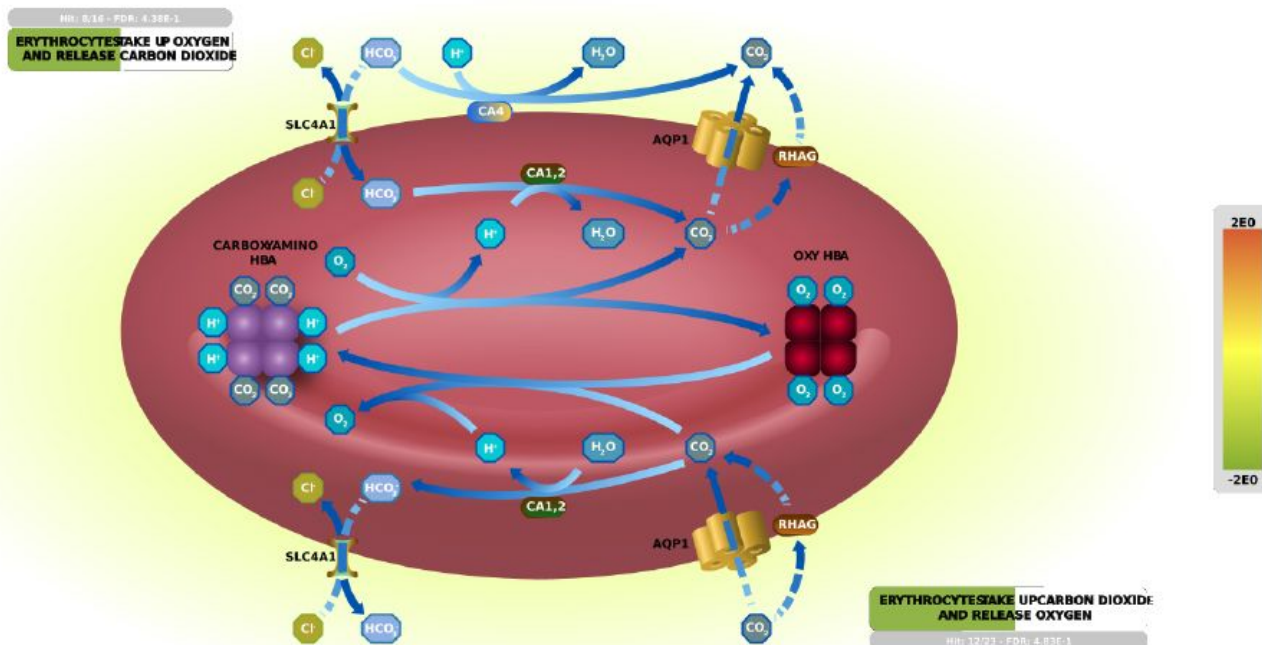


Figure 4

Enhanced high-level Reactome pathway diagram for O₂/CO₂ exchange in erythrocytes 48 by expression overlay with the MGI RNA-seq Post7 dataset. This high-level diagram represents two subpathways, namely erythrocyte take up oxygen and release carbon dioxide and erythrocyte take up carbon dioxide and release oxygen. The green band indicates the proportion of the pathway that is represented in the MGI RNA-seq Post7 dataset, and the colour (green) represents the down-regulation of the pathway genes. The grey bar contains the information for the number of pathway entities in the query dataset, the total number of the pathway entities, and the FDR corrected over-representation probability.

Supplementary Files

This is a list of supplementary files associated with this preprint. Click to download.

- [SupplementaryData112.zip](#)
- [WangetalSupplementaryInformation.pdf](#)